oxycholate, 1.0 mmol/L EDTA, 1.0 mmol/L Tris-HCl [pH 8.1]) and Tris-EDTA buffer. Immunoprecipitated chromatin fragments were eluted with elution buffer (1% sodium dodecyl sulfate, 100 mmol/L NaHCO3, 10 mmol/L dithiothreitol), and reverse cross-linked by incubating for 6 hours at 65°C in elution buffer containing 200 mmol/L NaCl. DNA fragments were purified and quantified by real-time detection PCR with primers for putative ISRE in the 2′5′OAS promoter region (forward, 5′-AAA TGC ATT TCC AGA GCA GAG TTC AGA G-3′, reverse, 5′-GGG TAT TTC TGA GAT CCA TCA TTG ACA GG-3′) or putative FBE in the Socs3 promoter region (forward, 5′-TGC TGC GAG TAG TGA CTA AAC ATT ACA AG -3′, reverse, 5′-AGC GGA GCA GGG AGT CCA AGT C -3′). Values were normalized by the measurement of input DNA.

pH77S.3/GLuc2A

pH77S.2 is a modification of pH77S[2] containing an additional mutation within the E2 protein (N476D in the polyprotein) that promotes infectious virus yields from RNA-transfected cells (Yi et al, unpublished data). To monitor replication, the GLuc sequence, fused at its C terminus to the foot-and-mouth disease virus 2A autoprotease, was inserted between p7 and NS2 of pH77S.2 (Supplementary Figure 4). To insert the GLuc-coding sequence between p7 and NS2 in pH77S.2, followed by the foot-and-mouth disease virus 2A protein-coding sequence, Mlu I, EcoR V, and Spe I restriction sites were created between the p7 and NS2 coding sequences by site-directed mutagenesis. DNA coding for GLuc was subcloned into the Mlu I and EcoR V sites of the modified plasmid after PCR amplification using the primers: 5′- ATA ATA TTA CGC GTA *TGG GAG TCA AAG TTC TGT TTG CC*-3′ (sequence corresponding to the N-terminal GLuc is italicized and that corresponding to Mlu I is underlined) and 5′-ATA AAT AGAT ATC *GTC ACC ACC GGC CCC CTT GAT CTT*-3′ (C terminal GLuc is italicized and EcoR V is underlined). A DNA fragment encoding the 17 amino acids of the foot-and-mouth disease virus 2A protein was generated by annealing the following complementary oligonucleotides: 5′- ATA TGA TAT CAA CTT TGA CCT TCT CAA GTT GGC CGG CGA CGT CGA GTC CAA CCC AGG GCC CAC TAG CAT AT-3′ and 5′-ATA TGC TAG TGG GCC CTG GGT TGG ACT CGA CGT CGC CGG CCA ACT TGA GAA GGT CAA AGT TGA TAT CAT AT-3′ (underlined sequences indicate EcoR V and Spe I sites). The annealed oligonucleotides were digested by both restriction enzymes and the product inserted into the corresponding sites of pH77S.2 containing GLuc to generate pH77S.2/GLuc2A. Q41R is a cell-culture adaptive mutation within the NS3 protease domain of pH77S. Because it is not essential for production of infectious virus (Yi et al, unpublished data), pH77S.2 and pH77S.2/GLuc2A constructs underwent this mutation by site-directed mutagenesis of a PCR fragment spanning the Afe I and BsrG I sites to replace Gln_{41} with wild-type Arg. The resulting plasmids (pH77S.2/R41Q and pH77S.2/GLuc2A/R41Q) were redesignated pH77S.3 and pH77S.3/GLuc2A, respectively.[3,4] GLuc has several advantages over other luciferase reporter enzymes in that it is smaller and allows more sensitive detection than either firefly or Renilla luciferase.[3,4] In addition, a signal sequence directs its secretion into cell-culture media, allowing real-time dynamic measurements of GLuc expression without the need for cell lysis. H77S.3/GLuc2A RNA produces infectious virus, although with lower efficiency than H77S.3 RNA (10-fold less).

References

1. Shimbo K, Kubo S, Harada Y, et al. Automated precolumn derivatization system for analyzing physiological amino acids by liquid chromatography/mass spectrometry. Biomed Chromatogr 2009; 24:683–691.
2. Yi M, Villanueva RA, Thomas DL, et al. Production of infectious genotype 1a hepatitis C virus (Hutchinson strain) in cultured human hepatoma cells. Proc Natl Acad Sci U S A 2006;103:2310–2315.
3. Shetty S, Kim S, Shimakami T, et al. Hepatitis C virus genomic RNA dimerization is mediated via a kissing complex intermediate. RNA 2010;16:913–925.
4. Shimakami T, Welsch C, Yamane D, et al. Protease inhibitor-resistant hepatitis C virus mutants with reduced fitness from impaired production of infectious virus. Gastroenterology 2011; 140:667–675.

GASTROENTEROLOGY 2013;145:658–667

BASIC AND TRANSLATIONAL—LIVER

Thromboxane A_2 Synthase Inhibitors Prevent Production of Infectious Hepatitis C Virus in Mice With Humanized Livers

YUICHI ABE,[1,2] HUSSEIN HASSAN ALY,[1] NOBUHIKO HIRAGA,[3] MICHIO IMAMURA,[3] TAKAJI WAKITA,[4] KUNITADA SHIMOTOHNO,[5] KAZUAKI CHAYAMA,[3] and MAKOTO HIJIKATA[1,2]

[1]Institute of Virus Research, [2]Graduate School of Biostudies, Kyoto University, Kyoto, Japan; [3]Department of Gastroenterology and Metabolism, Applied Life Sciences, Institute of Biomedical and Health Sciences, Hiroshima University, Hiroshima, Japan; [4]Department of Virology 2, National Institute of Infectious Disease, Tokyo, Japan; [5]Research Institute, Chiba Institute of Technology, Chiba, Japan

See Covering the Cover synopsis on page 495.

BACKGROUND & AIMS: A 3-dimensional (3D) culture system for immortalized human hepatocytes (HuS-E/2 cells) recently was shown to support the lifecycle of blood-borne hepatitis C virus (HCV). We used this system to identify proteins that are active during the HCV lifecycle under 3D culture conditions. **METHODS:** We compared gene expression profiles of HuS-E/2 cells cultured under 2-dimensional and 3D conditions. We identified signaling pathways that were activated differentially in the cells, and analyzed their functions in the HCV lifecycle using a recombinant HCV-producing cell-culture system, with small interfering RNAs and chemical reagents. We investigated the effects of anti-HCV reagents that altered these signaling pathways in mice with humanized livers (carrying human hepatocytes). **RESULTS:** Microarray analysis showed that cells cultured under 2-dimensional vs 3D conditions expressed different levels of messenger RNAs encoding prostaglandin synthases. Small interfering RNA–mediated knockdown of thromboxane A2 synthase (TXAS) and incubation of hepatocytes with a TXAS inhibitor showed that this enzyme is required for production of infectious HCV, but does not affect replication of the HCV genome or particle release. The TXAS inhibitor and a prostaglandin I2 receptor agonist, which has effects that are opposite those of thromboxane A_2, reduced serum levels of HCV and inhibited the infection of human hepatocytes by blood-borne HCV in mice. **CONCLUSIONS: An inhibitor of the prostaglandin synthase TXAS inhibits production of infectious HCV particles in cultured hepatocytes and HCV infection of hepatocytes in mice with humanized livers. It therefore might be therapeutic for HCV infection.**

Keywords: Infectious Virus Particle; Lipid Mediator; Antiviral Drug.

Approximately 170 million people worldwide are infected with hepatitis C virus (HCV),[1] with the majority suffering from chronic hepatitis, cirrhosis, and/or hepatocellular carcinoma.[2] HCV currently is treated using a combination of polyethylene glycol–conjugated interferon and ribavirin, although no more than 60% of individuals adequately respond.[3] Recently, inhibitors of HCV nonstructural proteins have been developed as direct-acting antiviral agents to treat HCV effectively.[4–6] However, HCV often acquires resistance against treatment with direct-acting antiviral agents in cases of monotherapy.[7] Current efforts therefore are focused on better understanding the lifecycle of HCV to find the cellular target of novel anti-HCV drugs to use the options for multi-drug therapy.

A cell-culture system that allows the production of recombinant infectious HCV (HCVcc) recently was developed using a cloned HCV genome and the hepatocellular carcinoma–derived Huh-7 cell line.[8–10] Experiments using the culture system have provided novel insights on the HCV lifecycle such as finding the production of infectious HCV particles near lipid droplets (LDs) and endoplasmic reticulum–derived LD-associated membranes.[11] Huh-7 cells, however, only allow the proliferation of recombinant HCV, and not blood-borne HCV (bbHCV).

To study the lifecycle of bbHCV, we cloned immortalized human hepatocyte HuS-E/2 cells, which permitted some degree of bbHCV infection.[12] Integrating hollow fibers into the 3-dimensional (3D) culture system resulted in efficient continuous proliferation of infected HCV production from the cells.[13] By using the improved system, we previously compared the gene expression profiles of HuS-E/2 cells under the 2-dimensional (2D) and 3D culture conditions using microarray analysis. This allowed us to identify signaling pathways that contribute to the proliferation of HCV, for example, peroxisome proliferator–activated

Abbreviations used in this paper: 2D, 2-dimensional; 3D, 3-dimensional; AAC, arachidonic acid cascade; bbHCV, blood-borne hepatitis C virus; cAMP, cyclic adenosine monophosphate; COX, cyclooxygenase; HCV, hepatitis C virus; HCVcc, hepatitis C virus from cell culture; IP, prostaglandin I_2 receptor; LD, lipid droplet; mRNA, messenger RNA; PG, prostaglandin; PGIS, prostaglandin I_2 synthase; RT-PCR, reverse-transcription polymerase chain reaction; qRT-PCR, quantitative reverse-transcription polymerase chain reaction; siRNA, small interfering RNA; TP, thromboxane A_2 receptor; TXA_2, thromboxane A_2; TXAS, thromboxane A_2 synthase; TXB_2, thromboxane B_2.

0016-5085/$36.00
http://dx.doi.org/10.1053/j.gastro.2013.05.014

receptor α signaling, which enhances HCV replication.[14] This result was confirmed by other groups,[15,16] corroborating that our strategy can uncover cellular events that support the proliferation of HCV. We therefore hypothesized that leveraging the in vitro systems described earlier may help elucidate the molecular mechanisms underlying the HCV lifecycle.

Prostanoids are metabolites of the arachidonic acid cascade (AAC) that possess various physiologic activities.[17] These metabolites include prostaglandin (PG) E_2, D_2, I_2, and F_2, and thromboxane A_2 (TXA_2).[17] Although several studies have shown that PG signaling contributes to liver regeneration,[18,19] the physiologic functions of these lipid mediators in human hepatocytes still are unknown. Interestingly, one report showed that PGE_2 might support HCV genome replication in cells bearing self-replicating HCV subgenomic replicon RNA.[20] Whether prostanoids are involved in the HCV lifecycle, however, has not been precisely investigated.

In this study, we provide evidence that TXA_2 synthase (TXAS) is involved in the formation of infectious HCV, by cell culture system, and that a TXAS inhibitor and PGI_2 receptor (IP) agonist that has opposite physiological effects to TXA_2 can be used as a novel anti-HCV drug by using chimeric mice bearing transplanted human hepatocytes.[21] This report shows the contribution of the AAC to HCV infectivity and the potency of a prostanoid as an antiviral agent.

Materials and Methods

Cell Culture

The human hepatocellular carcinoma-derived Huh-7 and Huh-7.5 cell lines were cultured as described previously.[22] HuS-E/2 cells are immortalized human hepatocytes transduced with *E6* and *E7* genes of human papilloma virus 18 and human telomerase reverse-transcription gene as described previously.[12] The 2D and 3D culture conditions for HuS-E/2 cells were as described previously.[12]

Reagents and Antibodies

FR122047, PGH_2, ONO1301, daltroban, and dibutyryl cyclic adenosine monophosphate (cAMP) sodium salt were purchased from Sigma-Aldrich (St. Louis, MO). Cyclooxygenase (COX)-2 inhibitor 1 and Ozagrel were purchased from Santa Cruz Biotechnology (Santa Cruz, CA). U-46619 was purchased from Cayman Chemical (Ann Arbor, MI). Beraprost was a generous gift from Toray, Co (Tokyo, Japan). FR122047, PGH_2, ONO1301, Daltroban, COX-2 inhibitor 1, Ozagrel, Beraprost, and calcium ionophore were dissolved in dimethyl sulfoxide. U-46619 and thromboxane B_2 (TXB_2) were dissolved in methyl acetate. Dibutyryl cAMP was dissolved in water. The effect of each reagent on cell viability was analyzed using a Cell Proliferation Kit 2 (Roche, Basel, Switzerland) based on the manufacturer's instructions. An antibody specific for core protein (antibody 32-1) was a gift from Dr Michinori Kohara (Tokyo Metropolitan Institute of Medical Science, Tokyo, Japan). Rabbit polyclonal anti-NS5A protein CL1 antibody and anti-HCV protein antibody in human serum were described previously.[11]

Microarray Analysis

Total RNA purified from HuS-E/2 cells cultured under 2D or 3D conditions in the absence of HCV infection was analyzed with a 3D-Gene Human Chip 25k (Toray, Co) to compare gene expression profiles as described previously.[14] The accession number of the results is listed as "E-MTAB-1491" in ArrayExpress.

Production of HCVcc and Sample Preparation

HCVcc was produced from the Huh-7 or Huh-7.5 cells transfected with in vitro synthesized Jikei Fulminant Hepatitis (JFH) 1^{E2FL} or J6/JFH1 RNA as described previously.[11] The transfected cells and culture medium were harvested at 4 days post-transfection. For $JFH1^{E2FL}$ RNA-transfected Huh-7 cells treated with TXAS-specific small interfering RNA (siRNA), cells and culture medium were harvested 3 days after transfection. Culture medium including HCVcc was concentrated and used for infection experiments as described previously.[11] Concentrated culture medium from JFH1 RNA-transfected Huh-7 cells was fractionated as described previously.[11] The infectivity titer in each fraction was analyzed by focus-formation assay, which was determined by the average number of HCV-positive foci.

Reverse-Transcription Polymerase Chain Reaction and Quantitative Reverse-Transcription Polymerase Chain Reaction

Total RNA was isolated from the cells and medium using Sepasol I Super and Sepasol II (Nacalai Tesque, Kyoto, Japan), respectively, according to the manufacturer's instructions. By using 200 ng of total RNA as a template, we performed reverse-transcription polymerase chain reaction (RT-PCR) and quantitative RT-PCR (qRT-PCR) with a 1-step RNA PCR kit and a 1-step SYBR Primescript RT-PCR kit 2 (Takara, Shiga, Japan), respectively, according to the manufacturer's instructions. Information on both experiments is shown in Supplementary Tables 1 and 2.

Infection of HCVcc

Infection experiments of HCVcc and detection of infected Huh-7.5 cells by indirect immunofluorescence analysis were performed mainly as described previously.[11] The number of infection-positive cells detected in 4×10^4 target cells 1 day after infection with HCVcc including 10^7 copies of RNase-resistant HCV genome was defined as the specific infectivity in the infection experiments in our protocol.

Indirect Immunofluorescence Analysis

HCV proteins were examined in cells using a Leica SP2 confocal microscope (Leica, Heidelberg, Germany), and infected cells were counted using a BioZero fluorescence microscope (Keyence, Tokyo, Japan).

Preparation of Intracellular HCV Particles

Intracellular HCV particles were prepared as described previously.[23]

Pharmacologic Test in Chimeric Mice Bearing Transplanted Human Hepatocytes

All mouse studies were conducted at Hiroshima University (Hiroshima, Japan) in accordance with the guidelines of the local committee for animal experiments. Chimeric mice

transplanted with human hepatocytes were generated as described previously.[21] The experimental protocol was approved by the Ethics Review Committee for Animal Experimentation of the Graduate School of Biomedical Sciences (Hiroshima University). The reagents were first administered 1 week after the chimeric mice were infected with a 1.0×10^5 titer of bbHCV. ONO1301 was injected subcutaneously at a dose of 200 μg/mouse. Beraprost and Ozagrel were administrated orally at a dose of 10 and 300 μg/mouse, respectively. For a positive control experiment, telaprevir was administered as described previously.[24] All reagents were administrated twice each day. Serum samples were collected at 2, 3, and 4 weeks after starting the treatments. HCV-RNA levels in the samples were evaluated in qRT-PCR.

Statistical Analyses of Data

The significance of differences in the means was determined by the Student *t* test (Figures 1-6, and Supplementary Figures 1-13) or the Wilcoxon signed-rank test (Figure 7 and Supplementary Figure 14).

Results

Expression of PG Synthase messenger RNA in HuS-E/2 Cells Cultured Under 3D Conditions

To identify signaling pathways that contribute to HCV proliferation under the 3D culture conditions, we compared the gene expression profiles of 2D- and 3D-cultured HuS-E/2 cells as described previously.[14] We found that the expression of 984 genes was up-regulated more than 2 times in both of 2 types of 3D-cultured HuS-E/2 cells, and expression of 1491 genes was down-regulated less than half the time. For the two 3D conditions, we identified the expression of a set of genes encoding enzymes of the AAC. The expression levels of messenger RNAs (mRNAs) for AAC enzymes, COX1, PGD_2 synthase, and TXAS increased in HuS-E/2 cells cultured under 3D conditions (Figure 1*A*), whereas those for PGE_2 and PGI_2 synthases (PGIS) decreased (Figure 1*A*). These results were confirmed by qRT-PCR analysis (Figure 1*A*, gray bars). The relative protein levels of those enzymes in 2D- and 3D-cultured HuS-E/2 cells reflected the quantitative difference of those mRNAs, except PGD_2 synthase (PGDS) (Figure 1*B*). The expression of those genes and the production of those proteins also were observed in the liver tissues from patients with hepatitis C, suggesting the functional roles of those products in the human liver (Supplementary Figure 1).

The AAC Contributes to Infectious HCV Production

To assess whether the AAC plays a role in the HCV lifecycle, the contributions of the AAC rate-limiting enzymes COX1 and COX2 were examined using the JFH1 cell culture system. We first investigated the role of COX1, which is known to be a constitutively expressed gene in general, by adding the COX1 inhibitor FR122047 to JFH1-RNA-transfected cell cultures. Even at higher concentrations, FR122047 did not markedly affect the amount of HCV RNA in the medium or cells (Figure 2*A*, black and white bars) with a little cytotoxicity at 10 μmol/L. Nevertheless, FR122047 dose-dependently decreased the infectivity of HCVcc in the culture medium (Figure 2*B* and *C*). Because the infection experiment using a lower titer of HCVcc from inhibitor-treated cells showed that the inhibitor affected the number of foci, but not the number of cells in a focus (Figure 2*C*), the treatment of COX1 inhibitor seemed to decrease the focus-forming ability of HCVcc. Next, the contribution of inducible COX2 was examined using COX2 inhibitor 1.

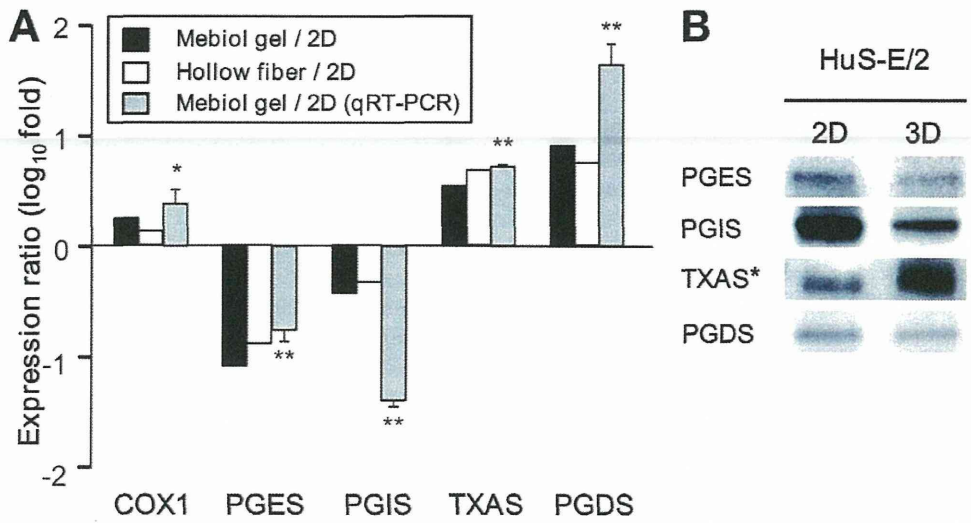

Figure 1. PG synthase mRNA expression under 3D culture conditions. (*A*) Results of microarray analysis. Black and white bars represent mRNA expression levels in HuS-E/2 cells cultured with Mebiol gel and hollow fibers, respectively, relative to levels observed in cells cultured under 2D conditions. Gray bars represent mRNA expression levels in HuS-E/2 cells cultured with Mebiol gel (Mebiol, Hiratuka, Japan) by quantifying with qRT-PCRs. qRT-PCR data show the averages from quadruplicate samples in 2 independent experiments ± SD. *Differs from control, $P < .01$; **differs from control, $P < .001$. (*B*) Protein levels of TXAS and various PG synthases in 2D-cultured and 3D-cultured HuS-E/2 cells. PG synthases except for TXAS were detected in whole-cell lysate. Asterisks show the result in membrane fraction.

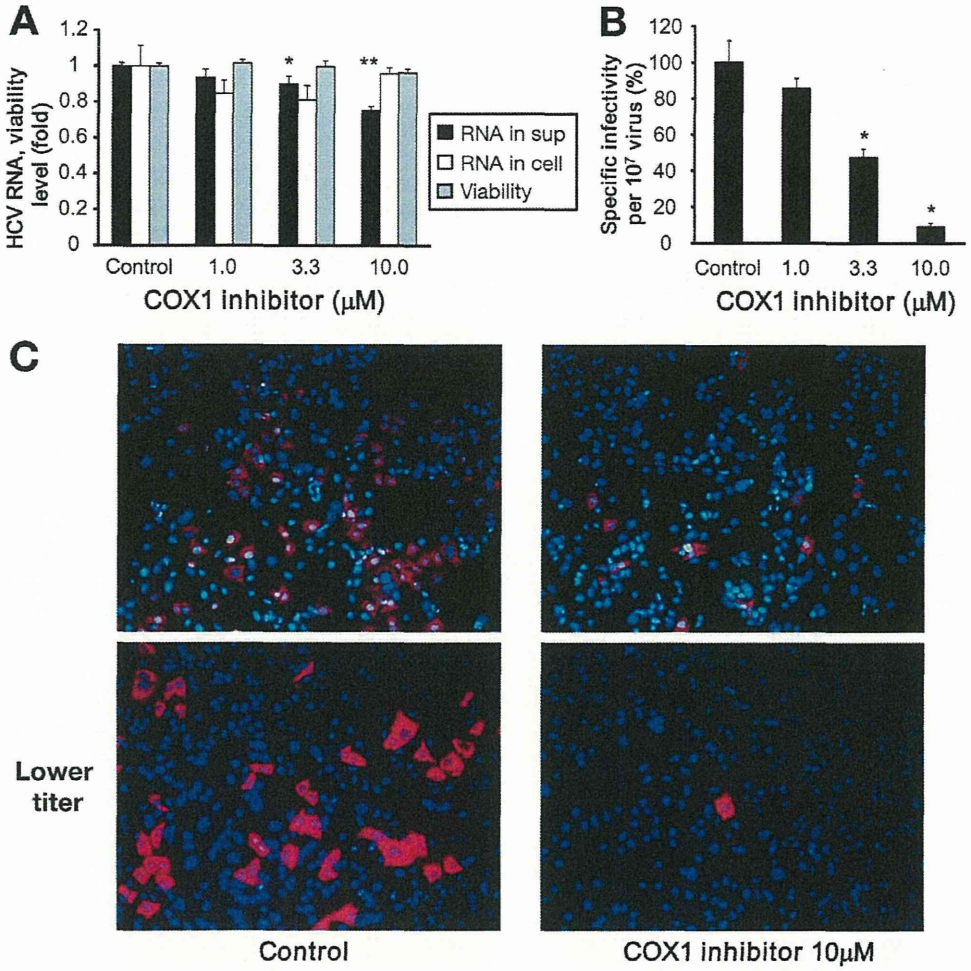

Figure 2. Effects of FR122047 on HCVcc-producing Huh-7 cells. (*A*) Effects of FR122047 on HCV-RNA levels in cultured HCVcc-producing cells. HCV RNA was collected from the medium (black bars) and cells (white bars), which were treated with FR122047 at the indicated concentrations. Mean cell viability ± SD for each sample condition also is plotted (gray bars). Averages from quadruplicate samples in 2 independent experiments ± SD are shown. (*B*) Effects of FR122047 on the infectivity of HCVcc produced using this cell-culture system. (*C*) FR122047 reduces infectious HCVcc in the culture medium. Huh-7.5 cells infected with HCVcc from the culture medium of cells treated with (*right panel*) and without (*left panel*) FR122047 at the indicated concentrations were stained with anti-HCV antibodies (magenta) and the nuclear stain 4′,6-diamidino-2-phenylindole (cyan). *Lower panels*: infected cells at a lower titer of inoculums. *Differs from control, $P < .01$; **differs from control, $P < .001$.

The inhibitor, however, did not affect the infectivity of HCVcc in the medium (Supplementary Figure 2*A* and *B*), probably because of the lack of *COX2* gene expression in Huh-7 cells (Supplementary Figures 2*C* and 3*A*). These data suggest that COX1 and the AAC play a role in infectious HCVcc production without significant effects on HCV genome replication or particle release from the cells.

TXAS Plays a Key Role in Infectious HCV Production

To further examine the contribution of the AAC to infectious HCVcc production, we focused on TXAS, because, similar to COX1 mRNA, TXAS mRNA levels increased in HuS-E/2 cells cultured under 3D conditions. Although PGD_2 synthase mRNA levels also increased, this synthase was unlikely to contribute to these processes because we did not detect PGD_2 synthase mRNA in Huh-7 cells in the JFH1 cell culture system (Supplementary Figure 3*A*). By using siRNA- and short hairpin RNA-mediated suppression of mRNA expression, we found that reducing TXAS mRNA levels in HCVcc-producing Huh-7 cells did not significantly affect the amount of HCV RNA in the medium or cells (Figure 3*B* and Supplementary Figure 4*B*, black and white bars), whereas HCVcc in the medium was less infectious, as was observed when the cells were treated with FR122047 (Figure 3*C* and Supplementary Figure 4*C*). Treatment with the TXAS inhibitor Ozagrel also dose-dependently suppressed infectious HCVcc production without significantly affecting HCV-RNA levels in the medium or cells (Figure 3*D* and *E*). Similar effects of Ozagrel were observed in another HCV cell culture system using Huh-7.5 cells and chimeric recombinant J6/JFH1 HCV, which encoded different structural proteins from JFH1[9] (Supplementary Figure 5), indicating that our results were not specific to the JFH1 cell culture system. Furthermore, treatment with PGH_2, a product of COX1 and a substrate of TXAS, was shown to increase the infectivity of HCVcc without effect on the HCV replication and egression despite the short half-life of PGH_2 (Supplementary Figure 6). These data suggest that the AAC, in particular TXAS activity and probably TXA_2 produced from PGH_2 by TXAS activity, contributes to infectious HCV production.

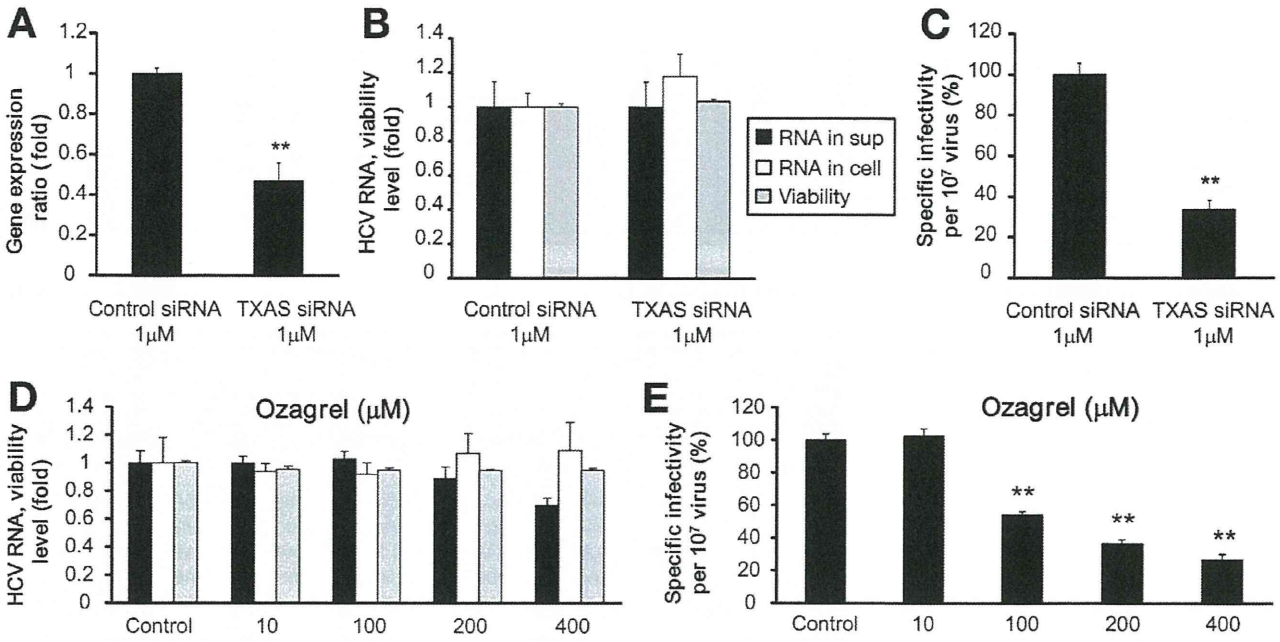

Figure 3. Effect of TXAS on infectious HCV production. (*A*) siRNA-mediated knockdown of TXAS mRNA expression. (*B*) Effects of TXAS-specific siRNA on HCV-RNA levels in the HCVcc-producing cell-culture system. (*C*) Effects of control and TXAS-specific siRNA on the infectivity of HCVcc in medium obtained from HCVcc-producing cell cultures were assessed. (*D*) Effects of Ozagrel on HCV-RNA levels were assessed in HCVcc-producing cell cultures. (*E*) Effects of Ozagrel on the infectivity of HCVcc produced from the cell-culture system were assessed. **Differs from control, $P < .001$.

TXA_2 Receptor Is Not Required for TXAS-Dependent Regulation of Infectious HCV Production

TXA_2 exerts its physiologic functions through the TXA_2 receptor (TP) on plasma membranes.[17] To examine the contribution of TXA_2/TP signaling, we investigated the effects of the TP agonist U-46619 in our system. Regardless of dose, however, U-46619 did not affect infectious HCVcc production in the culture system (Supplementary Figure 7). Treating Huh-7–derived cell lines with the TP agonist did not increase the calcium ion concentration—a major downstream effect of TXA_2/TP signaling—even though the activity of U-46619 was confirmed in HEK293 cells[17] (Supplementary Figure 8*A*). We also evaluated the activity of U-46619 in terms of TP-dependent activation of Rho and observed the Rho-dependent stress fiber formation induced with U-46619 in HEK293 cells (Supplementary Figure 8*B*). In addition,

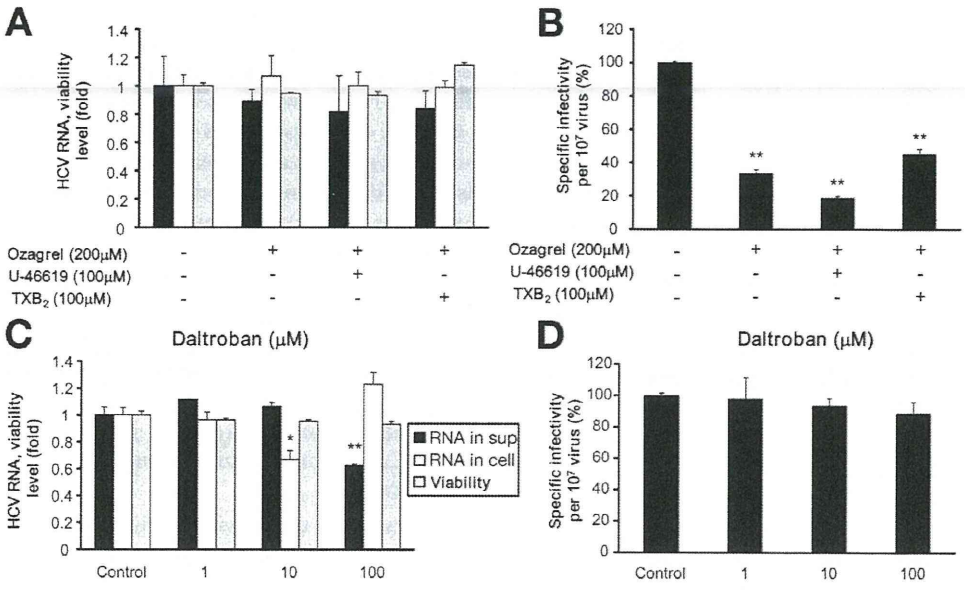

Figure 4. Role of TP in infectious HCVcc-producing cell cultures. (*A*) Effects of U-46619 and TXB_2 on HCV-RNA levels in HCVcc-producing cell cultures in the presence of Ozagrel were assessed. (*B*) The infectivity of HCVcc in culture medium from HCVcc-producing cells treated with U-46619 or TXB_2 in the presence of Ozagrel was assessed. (*C*) Effect of daltroban on HCV-RNA levels in HCVcc-producing cell cultures. (*D*) The infectivity of HCVcc in culture medium from HCVcc-producing cells treated with daltroban. *Differs from control, $P < .01$; **differs from control, $P < .001$.

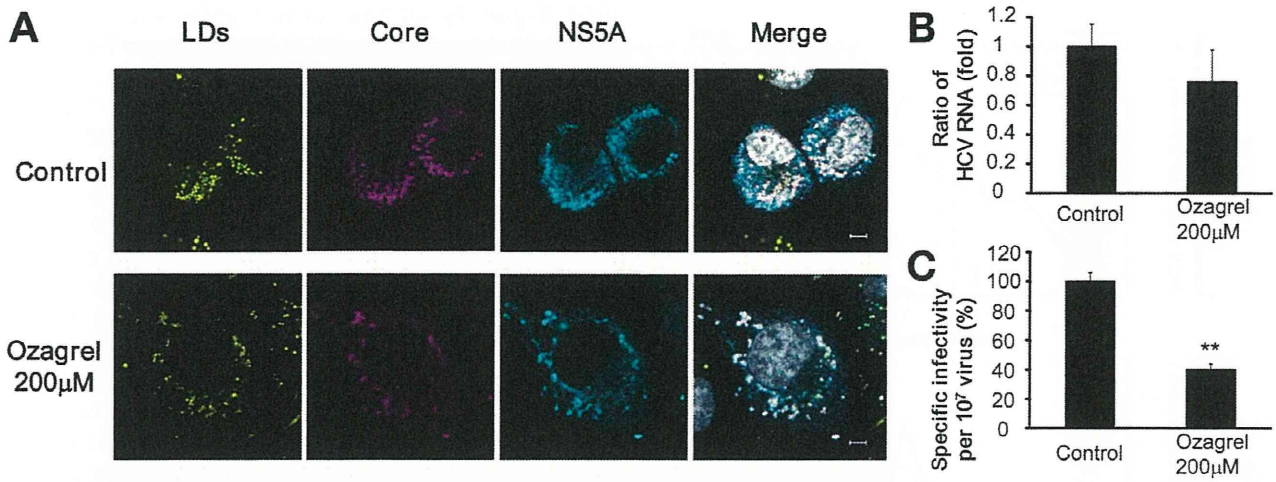

Figure 5. Core and NS5A near LDs and the quantity and infectivity of intracellular HCVcc. (*A*) HCV core (magenta) and NS5A (cyan) around LDs (yellow) in HCVcc-producing cells treated with the indicated reagents were observed using immunofluorescence analysis. Nuclei were stained with 4′,6-diamidino-2-phenylindole (gray). Scale bars, 5 μm. (*B*) Levels of intracellular HCV RNA obtained from the cells treated with Ozagrel. (*C*) The infectivity of intracellular HCV from cells treated with Ozagrel. Averages of triplicate samples from 2 independent experiments ± SD are shown. **Differs from control, $P < .001$.

the level of TP mRNA was, if any, quite low in human hepatocyte-derived cells and primary human hepatocytes, although only a small amount of the mRNA was detected in HuS-E/2 cells (Supplementary Figure 3*B*). These data suggest that TXA_2/TP signal transduction is deficient in Huh-7–derived cell lines.

To determine whether TP on the Huh-7 cells was saturated with endogenous TXA_2 ligand, we examined the effects of U-46619 in the presence of Ozagrel. U-46619, however, did not rescue the Ozagrel-mediated suppression of infectious HCVcc production (Figure 4*A* and *B*). In addition, the TP antagonist daltroban did not affect infectious HCVcc production (Figure 4*C* and *D*). These data indicate that TP-mediated signaling is not involved in TXAS-dependent regulation of infectious HCVcc production. In addition, we examined whether TXB_2—a stable metabolite of TXA_2 that does not activate TP—could be used to replace TXAS during infectious HCVcc production. TXB_2 did not counteract the effects of Ozagrel (Figure 4*A* and *B*), and did not by itself affect the HCV lifecycle (Supplementary Figure 7). These data suggest that TXA_2 or an unidentified metabolite of TXA_2 acts as a TP-independent regulator of infectious HCV production (see Discussion section).

TXAS-Derived Signaling Contributes to HCV Infectivity

A previous study showed that infectious HCV is produced near LDs, to which HCV proteins are recruited.[6] As shown in Figure 5*A*, inhibiting TXAS did not markedly affect the locations of the viral proteins core and NS5A around LDs, suggesting that TXAS-derived signaling does not contribute to the recruitment of HCV proteins to the LDs. Next, to examine whether TXAS-mediated signaling drives the egression of infectious HCVcc from the cells, we analyzed intracellular HCVcc in cells treated with Ozagrel. Levels of intracellular HCVcc RNA in Huh-7 cells treated with or without Ozagrel were equivalent (Figure 5*B*). Nevertheless, the infectivity of intracellular HCVcc from the cells treated with Ozagrel was decreased markedly, as was that of HCVcc in the medium (Figure 5*C*). This result indicated that TXAS-derived signaling is not involved in the release of infectious HCV particles. Taken together, it seems likely that TXAS-derived signaling plays a role in infectious particle formation in the cells.

Inhibition of TXAS Changes the Physicochemical Properties of HCVcc

We next analyzed HCVcc produced from cells treated with Ozagrel using sucrose density gradient ultracentrifugation. As reported previously,[11] 2 types of fractions containing either highly infectious, low-density HCVcc (peak fraction, 6) or less infectious, high-density HCVcc (peak fraction, 5) were obtained using samples derived from cells without treatment with Ozagrel, indicating that infectious HCVcc was present mainly in fraction 6 (Figure 6, white bars, upper and lower panels). On the other hand, analyzing Ozagrel-treated cells showed decreased levels of HCV RNA in fraction 6 (Figure 6, solid lines, upper and lower panels). Of note, the amount of HCV RNA in fraction 5 remained similar with or without Ozagrel treatment (Figure 6, lower panel). These results suggest that inhibition of TXAS-mediated signaling changes the physicochemical characteristics of HCVcc, resulting in altered infectivity.

A TXAS Inhibitor and IP Agonists Inhibit Early HCV Expansion in bbHCV-Infected Chimeric Mice

Finally, we examined the in vivo anti-HCV effects of a TXAS inhibitor using bbHCV and urokinase plasminogen activator/severe combined immunodeficiency mice bearing transplanted human hepatocytes. The IP

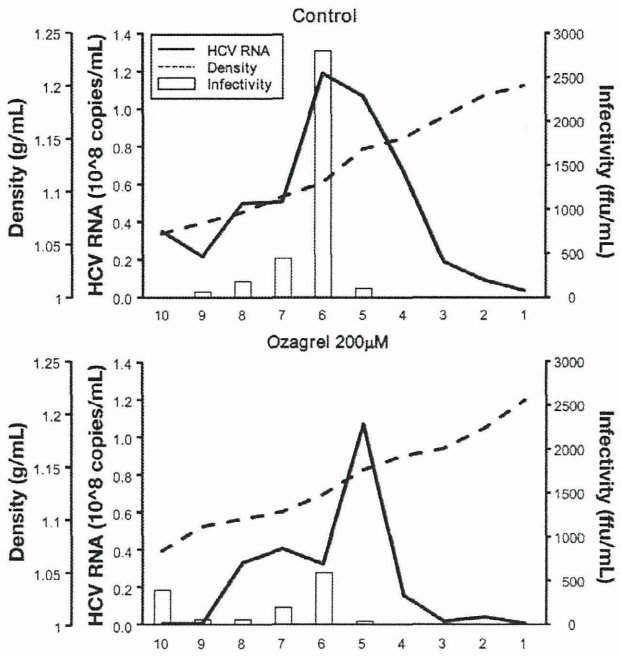

Figure 6. Buoyant density of HCVcc produced from cells treated with Ozagrel. *Lower* and *upper panels* show the results of HCVcc from the cells with and without Ozagrel treatment, respectively. HCV RNA (*solid line*), fraction density (*dotted line*), and HCV infectivity (*white bars*) in each fraction collected after ultracentrifugation are shown. Representative results from 2 independent experiments are shown.

agonist Beraprost also was tested because PGI_2 produces effects opposite of TXA_2 during several physiologic processes, including vascular constriction in human beings.[25] Both drugs delayed the increase in serum levels of HCV RNA (Figure 7). Of note, even 4 weeks after treatment, Beraprost reduced serum HCV-RNA levels to less than a quarter of those observed in control mice (Figure 7). Our results indicate that these drugs may inhibit HCV proliferation in vivo, and that inhibition of TXAS-derived signaling and activation of IP-mediated PGI_2 signaling can control HCV proliferation. Although we examined the effects of the PGIS and IP agonist on the HCV lifecycle using the HCVcc-producing cell-culture system, Beraprost did not result in any notable changes (Supplementary Figure 9). To examine whether the Huh-7 cells respond to the IP agonist, we assessed cAMP signaling using a plasmid-bearing cAMP-responsive element in a promoter upstream of the luciferase gene; cAMP signaling is a major intracellular signaling pathway that is activated by IP agonists. The IP agonist, however, did not activate cAMP signaling in Huh-7 cells even though the pathway was activated in HuS-E/2 cells.

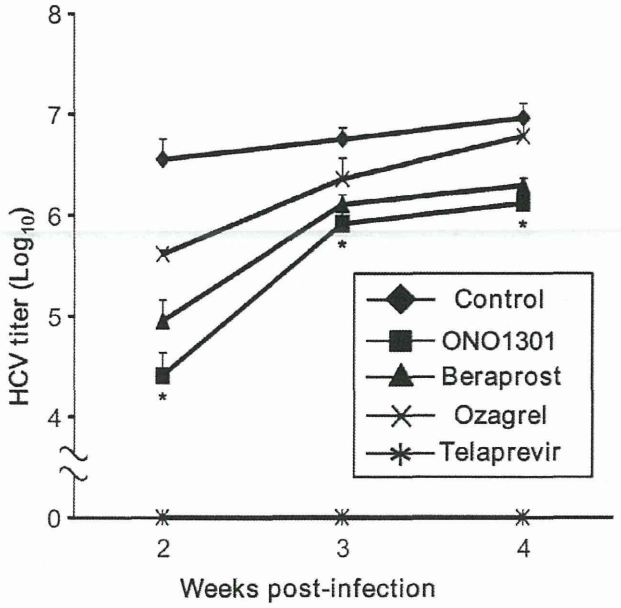

Figure 7. Effects of ONO1301, Beraprost, Ozagrel, and Telaprevir on the expansion of bbHCV-infected urokinase plasminogen activator/severe combined immunodeficiency mice bearing human hepatocytes. Data are presented as means ± SD for 6 (control, *diamonds*), 4 (ONO1301, *squares*; Ozagrel, *crosses*; Telaprevir, *asterisk*), and 3 (Beraprost, *triangles*) samples. *Differs from control, $P < .05$.

As another candidate anti-HCV drug, we examined the effect of ONO1301, possessing both TXAS-inhibitor and IP-agonist activities, in the humanized chimeric mouse. ONO1301 produced the most robust suppression of HCV infections (Figure 7). The effects of ONO1301 also were studied in the HCVcc-producing cell cultures, as with Ozagrel. ONO1301 suppressed infectious HCV production (Supplementary Figure 10), although ONO1301 did not activate cAMP signaling in Huh-7 cells (Supplementary Figure 11). A slight decrease of HCVcc egression, however, caused by the treatment with ONO1301 at high concentrations, might be of note. These results further supported our conclusion that TXAS-mediated signaling contributes to infectious HCV production, although the functional role of PGI_2 in this process still is unknown.

Discussion

In this study, we showed that TXAS is involved in the development of infectious HCV. Administration of a TXAS inhibitor inhibited early stages of HCV proliferation postinfection in a chimeric mouse model. These results suggest that TXAS-mediated infectious HCV production is a potential target for novel anti-HCV therapies.

We first found that inhibiting COX1 and TXAS decreased the infectivity of HCVcc in the culture medium without any significant effects on viral genome replication and particle egression (Figures 2 and 3). In addition, we showed that inhibition of TXAS did not affect the release of infectious HCVcc from the cells (Figure 5). Thus, we concluded that TXAS probably regulates HCV particle maturation and the development of infectivity. Knockdown of apolipoprotein E, heat shock protein 70, and annexin A2 expression was shown previously to inhibit infectious HCVcc production.[26] Of note, decreased expression of these host factors reduced the production of HCVcc in the culture medium as well as intracellular HCVcc levels in HCVcc-producing cells, suggesting that TXAS is playing a different role in HCVcc production.

BASIC AND TRANSLATIONAL LIVER

Moreover, our results suggest that TXAS is a host factor that contributes only to the development of HCV infectivity.

A previous study reported that infectious HCVcc is produced near LDs.[11] The HCV proteins core and NS5A are located on and nearby LDs, respectively, suggesting a role in the production of infectious HCVcc.[11] Because LD localization of these proteins was not affected by the TXAS inhibitor (Figure 5*A*), TXAS probably is required after these viral proteins are recruited to LDs.

Several studies have shown that the buoyant density of infectious HCVcc differs slightly from that of noninfectious HCVcc.[11,27,28] Infectious and noninfectious HCVcc are found in lower- and higher-density fractions, respectively. In the present study, inhibition of TXAS reduced the amount of HCVcc in the lower-density fraction (fraction 6) containing the infectious particles, whereas levels of primarily noninfectious HCVcc particles in the higher-density fraction (fraction 5) were not affected (Figure 6). These results mirrored previously reported data about NS5A mutant HCVcc, which do not produce infectious particles.[11] These results suggest that TXAS might be required to produce infectious HCVcc near the LDs.

Studies with treatment with methyl-β-cyclodextrin or lipoprotein lipase have shown that changing the physicochemical properties of HCVcc,[28–30] in which the peak density fraction containing HCVcc shifted higher, diminished the infectivity of the particles.[29,30] Because TXAS inhibitors did not show the apparent shift to a higher density (Figure 6), future molecular analyses of HCVcc particles should be required to reveal the underlying structural mechanisms for HCV infectivity.

Prostanoids play various physiologic functions, including regulatory roles in muscle and blood vessels.[17] Although inhibition of TXAS decreased the infectivity of HCVcc (Figure 3), the identity of the relevant prostanoid and how that product functions in the development of infectious HCV are currently unclear. Because the treatment of PGH_2, a substrate of TXAS, caused the increase of infectious HCV production (Supplementary Figure 6), it seemed likely that the decrease of HCV infectivity is not due to an accumulation of PGH_2 caused by TXAS inhibition. Although we analyzed the total fatty acids in the HCV-infected Huh-7.5 cells treated with and without Ozagrel, the compositions of fatty acids, including arachidonic acid, were not largely different from each other (Supplementary Figure 12, the arachidonic acid is shown as C20:4ω-6), suggesting that the effect of Ozagrel is not caused by major changes of fatty acid composition.

The activity of the TXAS product TXA_2 was not examined directly because its half-life is quite short.[31] Usually, TXA_2 activity is measured using stable agonists and antagonists of TP. We showed, however, that TP-mediated signaling is not related to the processes examined in the current study (Figure 4). It seemed likely that TXA_2 itself or an unidentified metabolite of TXA_2 mediates the development of HCV infectivity in a TP-independent manner. PGI_2 and the PGD_2 metabolite 15d-PGJ_2 have been identified as ligands of peroxisome proliferator activated receptor δ and γ, respectively.[32,33] Therefore, the TXAS product may act as a ligand of various nuclear receptors to regulate infectious HCV production. In primary human hepatocytes and liver of chimeric mice transplanted with human hepatocytes, the expression of human TP mRNA was not observed (Supplementary Figures 3*A* and 13), although it was detected in human liver tissue, consisting of many cell types (Supplementary Figure 13). It may be true, therefore, that the *TP* gene is not largely expressed in human hepatocytes in the liver as with Huh-7 cells. Taken together, it is probable that infectious HCV is produced in a TP-independent manner in human liver infected with HCV. Further studies regarding the TP-independent roles of TXAS products in hepatocytes may be required to elucidate the mechanisms of infectious HCV formation.

Recently, various drugs targeting viral proteins were developed, resulting in more HCV-specific therapeutic profiles than those of conventional drugs.[34] Monotherapy with an HCV-specific drug, however, sometimes fails to clear the HCV infection because of rapidly emerging resistant variants.[35] We found that a TXAS inhibitor and IP agonists suppressed early stage expansion of bbHCV postinfection of chimeric mice bearing human hepatocytes (Figure 7). These results clearly indicate that the TXAS inhibitor and IP agonist are novel candidates for anti-HCV drugs. In this experiment, the effects of an IP agonist and the TXAS inhibitor were compared because TXA_2 and IP agonists have opposite clinical effects.[20] This implies that the IP agonist may have suppressed the effects of TXAS in the bbHCV-infected transplanted human hepatocytes. Contrary to our expectations, however, neither siRNA-mediated knockdown of PGIS expression nor treatment with the IP agonist Beraprost affected HCV genome replication, particle egression, or HCVcc infectivity (Supplementary Figure 9). The responsiveness of Huh-7 cells to the IP agonist then was examined by monitoring activation of cAMP signaling, a pathway that normally is activated downstream of IP. The results show that Huh-7 cells were deficient in signaling from IP to intracellular cAMP production (Supplementary Figure 11). Although the therapeutic mechanism of action for the IP agonist in chimeric mice has not been clarified yet, the IP agonist may signal through IP to counteract TXA_2 signaling and suppress the effects of endogenous TXAS products on the formation of infectious HCV. In this in vivo experiment, the effect of drugs waned over time, especially in the case of Ozagrel. We examined the effect of Ozagrel on the secondary HCV propagation in the mice inoculated with the sera of the HCV infected mice treated with Ozagrel in the first drug treatment. The results showed that HCV proliferated in the secondarily infected chimeric mice irrespective of the treatment of Ozagrel (Supplementary Figure 14), suggesting that HCV proliferating in the chimeric mice with the first treatment

acquired the resistance against Ozagrel. We analyzed partial genomic sequences of the drug-resistant HCVs by the direct sequencing method. We found that 68 base substitutions, 10 of which were accompanied with amino acid substitution, were present in such HCV genomes, compared with those in the mice untreated with the drug (Supplementary Figure 15). This indicated that the HCV proliferating in the chimeric mouse treated with Ozagrel included a large number of base substitutions in the genome. Further study of such drug-resistant HCV, for example, the reverse genetic analysis using a recombinant HCV system, will help to reveal the molecular mechanisms of the medicinal effects of this drug and the infectious HCV production. Furthermore, these results show the need to find the optimum dose of TXAS inhibitor for effective therapy and to use this drug as one option with different action mechanisms for multidrug therapy.

Supplementary Material

Note: To access the supplementary material accompanying this article, visit the online version of *Gastroenterology* at www.gastrojournal.org, and at http://dx.doi.org/10.1053/j.gastro.2013.05.014.

References

1. Wasley A, Alter MJ. Epidemiology of hepatitis C: geographic differences and temporal trends. Semin Liver Dis 2000;20:1–16.
2. Younossi Z, Kallman J, Kincaid J. The effects of HCV infection and management on health-related quality of life. Hepatology 2007; 45:806–816.
3. Fried MW, Shiffman ML, Reddy KR, et al. Peginterferon alfa-2a plus ribavirin for chronic hepatitis C virus infection. N Engl J Med 2002; 347:975–982.
4. Gao M, Nettles RE, Belema M, et al. Chemical genetics strategy identifies an HCV NS5A inhibitor with a potent clinical effect. Nature 2010;465:96–100.
5. Chayama K, Takahashi S, Toyota J, et al. Dual therapy with the nonstructural protein 5A inhibitor, daclatasvir, and the nonstructural protein 3 protease inhibitor, asunaprevir, in hepatitis C virus genotype 1b-infected null responders. Hepatology 2012; 55:742–748.
6. Lin C, Kwong AD, Perni RB. Discovery and development of VX-950, a novel, covalent, and reversible inhibitor of hepatitis C virus NS3.4A serine protease. Infect Disord Drug Targets 2006;6:3–16.
7. Sarrazin C, Zeuzem S. Resistance to direct antiviral agents in patients with hepatitis C virus infection. Gastroenterology 2010; 138:447–462.
8. **Wakita T, Pietschmann T**, Kato T, et al. Production of infectious hepatitis C virus in tissue culture from a cloned viral genome. Nat Med 2005;11:791–796.
9. Lindenbach BD, Evans MJ, Syder AJ, et al. Complete replication of hepatitis C virus in cell culture. Science 2005;309:623–626.
10. **Zhong J, Gastaminza P**, Cheng G, et al. Robust hepatitis C virus infection in vitro. Proc Natl Acad Sci U S A 2005;102:9294–9299.
11. Miyanari Y, Atsuzawa K, Usuda N, et al. The lipid droplet is an important organelle for hepatitis C virus production. Nat Cell Biol 2007;9:1089–1097.
12. Aly HH, Watashi K, Hijikata M, et al. Serum-derived hepatitis C virus infectivity in interferon regulatory factor-7-suppressed human primary hepatocytes. J Hepatol 2007;46:26–36.
13. Aly HH, Qi Y, Atsuzawa K, et al. Strain-dependent viral dynamics and virus-cell interactions in a novel in vitro system supporting the life cycle of blood-borne hepatitis C virus. Hepatology 2009; 50:689–696.
14. Aly HH, Shimotohno K, Hijikata M. 3D cultured immortalized human hepatocytes useful to develop drugs for blood-borne HCV. Biochem Biophys Res Commun 2009;379:330–334.
15. Chockalingam K, Simeon RL, Rice CM, et al. A cell protection screen reveals potent inhibitors of multiple stages of the hepatitis C virus life cycle. Proc Natl Acad Sci U S A 2010;107:3764–3769.
16. Gastaminza P, Whitten-Bauer C, Chisari FV. Unbiased probing of the entire hepatitis C virus life cycle identifies clinical compounds that target multiple aspects of the infection. Proc Natl Acad Sci U S A 2010;107:291–296.
17. Bos CL, Richel DJ, Ritsema T, et al. Prostanoids and prostanoid receptors in signal transduction. Int J Biochem Cell Biol 2004; 36:1187–1205.
18. Little P, Skouteris GG, Ord MG, et al. Serum from partially hepatectomized rats induces primary hepatocytes to enter S phase: a role for prostaglandins? J Cell Sci 1988;91:549–553.
19. Rudnick DA, Perlmutter DH, Muglia LJ. Prostaglandins are required for CREB activation and cellular proliferation during liver regeneration. Proc Natl Acad Sci U S A 2001;98:8885–8890.
20. Waris G, Siddiqui A. Hepatitis C virus stimulates the expression of cyclooxygenase-2 via oxidative stress: role of prostaglandin E2 in RNA replication. J Virol 2005;79:9725–9734.
21. Tateno C, Yoshizane Y, Saito N, et al. Near completely humanized liver in mice shows human-type metabolic responses to drugs. Am J Pathol 2004;165:901–912.
22. Kushima Y, Wakita T, Hijikata M. A disulfide-bonded dimer of the core protein of hepatitis C virus is important for virus-like particle production. J Virol 2010;84:9118–9127.
23. Gastaminza P, Kapadia SB, Chisari FV. Differential biophysical properties of infectious intracellular and secreted hepatitis C virus particles. J Virol 2006;80:11074–11081.
24. Kamiya N, Iwao E, Hiraga N, et al. Practical evaluation of a mouse with chimeric human liver model for hepatitis C virus infection using an NS3-4A protease inhibitor. J Gen Virol 2010; 91:1668–1677.
25. Flavahan NA. Balancing prostanoid activity in the human vascular system. Trends Pharmacol Sci 2007;28:106–110.
26. Bartenschlager R, Penin F, Lohmann V, et al. Assembly of infectious hepatitis C virus particles. Trends Microbiol 2011;19:95–103.
27. Andre P, Komurian-Pradel F, Deforges S, et al. Characterization of low- and very-low-density hepatitis C virus RNA-containing particles. J Virol 2002;76:6919–6928.
28. Nielsen SU, Bassendine MF, Burt AD, et al. Association between hepatitis C virus and very-low-density lipoprotein (VLDL)/LDL analyzed in iodixanol density gradients. J Virol 2006; 80:2418–2428.
29. Aizaki H, Morikawa K, Fukasawa M, et al. Critical role of virion-associated cholesterol and sphingolipid in hepatitis C virus infection. J Virol 2008;82:5715–5724.
30. Shimizu Y, Hishiki T, Sugiyama K, et al. Lipoprotein lipase and hepatic triglyceride lipase reduce the infectivity of hepatitis C virus (HCV) through their catalytic activities on HCV-associated lipoproteins. Virology 2010;407:152–159.
31. Gryglewski RJ. Prostacyclin among prostanoids. Pharmacol Rep 2008;60:3–11.
32. Forman BM, Tontonoz P, Chen J, et al. 15-Deoxy-delta 12, 14-prostaglandin J2 is a ligand for the adipocyte determination factor PPAR gamma. Cell 1995;83:803–812.
33. Gupta RA, Tan J, Krause WF, et al. Prostacyclin-mediated activation of peroxisome proliferator-activated receptor delta in colorectal cancer. Proc Natl Acad Sci U S A 2000;97:13275–13280.
34. Pawlotsky JM, Chevaliez S, McHutchison JG. The hepatitis C virus life cycle as a target for new antiviral therapies. Gastroenterology 2007; 132:1979–1998.

35. Wohnsland A, Hofmann WP, Sarrazin C. Viral determinants of resistance to treatment in patients with hepatitis C. Clin Microbiol Rev 2007;20:23–38.

Author names in bold designate shared co-first authorship.

Received August 11, 2012. Accepted May 13, 2013.

Reprint requests

Address requests for reprints to: Makoto Hijikata, PhD, Laboratory of Human Tumor Viruses, Department of Viral Oncology, Institute for Virus Research, Kyoto University, 53, Kawaharacho, Shogoin, Sakyoku, Kyoto 606-8507, Japan. e-mail: mhijikat@virus.kyoto-u.ac.jp; fax: (81) 75-751-3998.

Acknowledgments

The authors thank Dr Michinori Kohara (Tokyo Metropolitan Institute of Medical Science, Tokyo, Japan) for providing anti-hepatitis C virus core antibody; Toyobo, Co (Osaka, Japan) for providing hollow fibers; Toray, Co (Tokyo, Japan) for providing Beraprost; and Dr Masayoshi Fukasawa (National Institute of Infectious Disease, Tokyo, Japan) for helpful discussion.

Present address of H.H.A.: Department of Virology 2, National Institute of Infectious Disease, Tokyo, Japan.

Transcript Profiling: The microarray data in this study was named "HuSE2, 2Dvs3D," and was registered in ArrayExpress. Accession number: E-MTAB-1491.

Nucleic acid sequences: Sequencing data in this study were named "BankIt1626925 Seq1" and "BankIt1626925 Seq3", and registered with GenBank. Accession numbers: KF006982 and KF006984, respectively.

Conflicts of interest

The authors disclose no conflicts.

Funding

Supported by grants-in-aid from the Ministry of Health, Labour and Welfare of Japan.

Supplementary Materials and Methods

Preparation of Subcellular Fraction and Protein Detection With Western Blotting

Subcellular fractions of HuS-E/2 cells and patient's tissues were prepared with the ProteoExtract Subcellular proteome Extraction Kit (Millipore, Billerica, MA) according to the manufacturer's protocol. Five micrograms of total protein of each fraction or whole-cell lysate of each cell was analyzed by Western blotting. Western blotting was performed as described previously.[1]

Collection of Total RNA and Cell Lysate From HCV-Infected Patients' Tissue

Total RNA from patients' tissue was collected with RNeasy mini (Qiagen, Hilden, Germany). In brief, frozen tissues were homogenized in lysis buffer with a Power Masher (Nippi, Tokyo, Japan). Homogenized samples were used for RNA purification according to the manufacturer's protocol. Cell lysate from tissues were collected with RIPA buffer (Thermo Scientific, Waltham, MA) or the ProteoExtract Subcellular proteome Extraction Kit according to the manufacturer's protocol.

cAMP Reporter Assay

Huh-7-derived and HuS-E/2 cells were transfected with pCRE-Luc (Agilent Technologies, Santa Clara, CA) using Fugene6 (Roche) and Effectene (Qiagen), respectively, essentially according to the manufacturers' protocols. Six hours and 2 days post-transfection of Huh-7-derived and HuS-E/2 cells, respectively, the culture medium was replaced with fresh medium containing one of the reagents. One and 3 day(s) post-transfection of Huh-7-derived and HuS-E/2 cells, respectively, luciferase activity in the cells was measured using a luciferase activity detection reagent (Promega, Madison, WI) and a Lumat LB 9507 luminometer (EG&G Berthold, Bad Wildbad, Germany).

Calcium Ion Quantification

HEK293, Huh-7-derived, and HuS-E/2 cells were treated with the calcium ionosphere A23187 (Sigma-Aldrich) and the TP agonist U-46619 for 1 day. Calcium ion concentrations were quantified using a calcium assay kit (Cayman Chemical) according to the manufacturer's protocols.

Actin Polymerization Assay

Activation of actin polymerization via TP was measured with fluorescein isothiocyanate-phalloidin (Sigma-Aldrich). After culture in lipid-free fresh medium, cells were stimulated with 10 μmol/L U46619 containing medium for 30, 60, and 180 seconds. Then, samples were stained with 10 μg/mL fluorescein isothiocyanate phalloidin, Fluorescent intensity at 520 nm was measured.

Fatty Acid Analysis

Fatty acid analysis of HCV-infected Huh-7.5 cells treated with or without Ozagrel was performed by Toray Research Center, Inc, Tokyo, Japan using gas chromatography. Total fatty acid samples were extracted from the cells according to the Bligh-Dyer[2] method.

Secondary Infection Experiments in Chimeric Mice Transplanted Human Hepatocytes

The chimeric mice were inoculated intravenously with patient serum including 1.0×10^5 genome titer of bbHCV (genotype 1b) as the first infection. Ozagrel was administered orally twice each day (300 μg/day) 1 week after the inoculation. The serum samples from those mice were collected at 5 weeks after starting the drug treatments, and used as inocula in the secondary infection experiment. Naive chimeric mice were inoculated with the collected chimeric mice serum including 1.0×10^5 genome titer of HCV. Administration of Ozagrel was started simultaneously. HCV-RNA levels in the blood of the chimeric mice at 1, 2, and 3 weeks after infection in secondary infection experiments were evaluated by qRT-PCR.

Determination of Nucleotide Sequence of HCV Genome After Treatment With Ozagrel

Chimeric mice were inoculated secondarily with sera from HCV-infected chimeric mice with or without Ozagrel treatment. Sera of these chimeric mice treated with or without Ozagrel were collected 5 weeks after the inoculation and the start of the treatment. HCV genome sequences of these samples were determined by the direct sequencing method according to the protocol described previously.[3] HCV genomic sequences obtained from sera of mice with 2 different types of treatment were compared with each other. Mice with 2 different types of treatments were as follows: first, mice inoculated secondarily with sera from the first chimeric mouse without treatment were not treated with the drug (BankIt1626925 Seq3 in GenBank). Second, mice inoculated secondarily with sera from the first chimeric mouse with treatment were treated with the drug (BankIt1626925 Seq1 in GenBank). These sequencing data were registered with GenBank (http://www.ncbi.nlm.nih.gov/genbank/).

Supplementary References

1. Kushima Y, Wakita T, Hijikata M. A disulfide-bonded dimer of the core protein of hepatitis C virus is important for virus-like particle production. J Virol 2010;84:9118-9127.
2. Bligh EG, Dyer WJ. A rapid method of total lipid extraction and purification. Can J Biochem Physiol 1959;37:911-917.
3. Kimura T, Imamura M, Hiraga N, et al. Establishment of an infectious genotype 1b hepatitis C virus clone in human hepatocyte chimeric mice. J Gen Virol 2008;89:2108-2113.

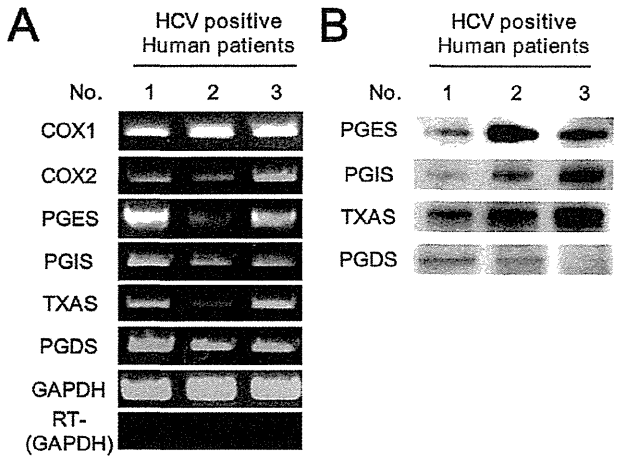

Supplementary Figure 1. Protein and mRNA levels of PG synthases in HCV-infected patient tissue. (*A* and *B*) mRNA expression and protein levels of PG synthases in HCV-infected patient tissue. Representative results from 2 independent experiments are shown.

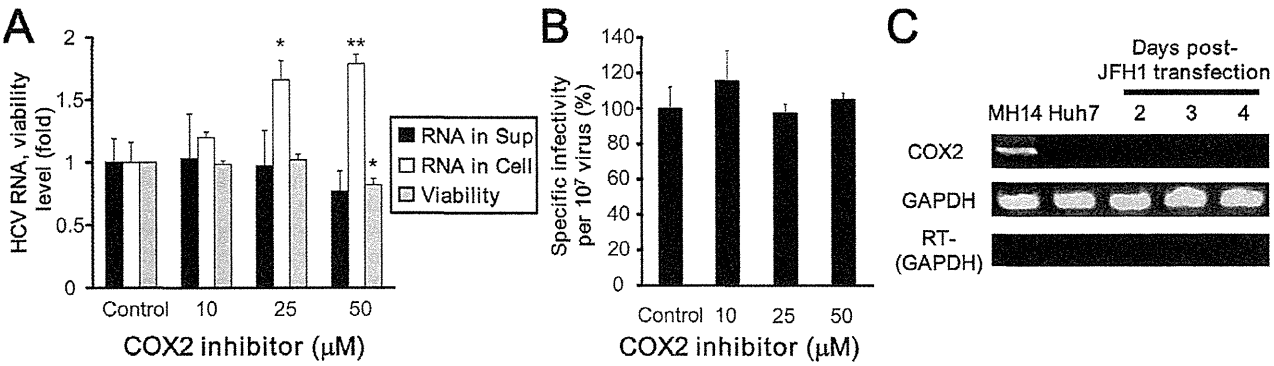

Supplementary Figure 2. Effects of COX2 inhibitor 1 on infectious HCV production. (*A*) Effects of COX2 inhibitor 1 on HCV-RNA levels in the HCVcc-producing cell-culture system. Levels of HCV RNA in medium (*black bars*) and cells (*white bars*) treated with or without COX2 inhibitor 1 were assessed with qRT-PCRs and plotted as amounts relative to results observed with control cells (control). Mean cell viability ± SD for each sample condition also is plotted (*gray bars*). (*B*) Effects of COX2 inhibitor 1 on the infectivity of HCVcc produced using the cell-culture system. (*C*) Expression of COX2 mRNA in MH14 (positive control), Huh-7, and JFH1-transfected Huh-7 cells. *Differs from control, $P < .01$; **differs from control, $P < .001$.

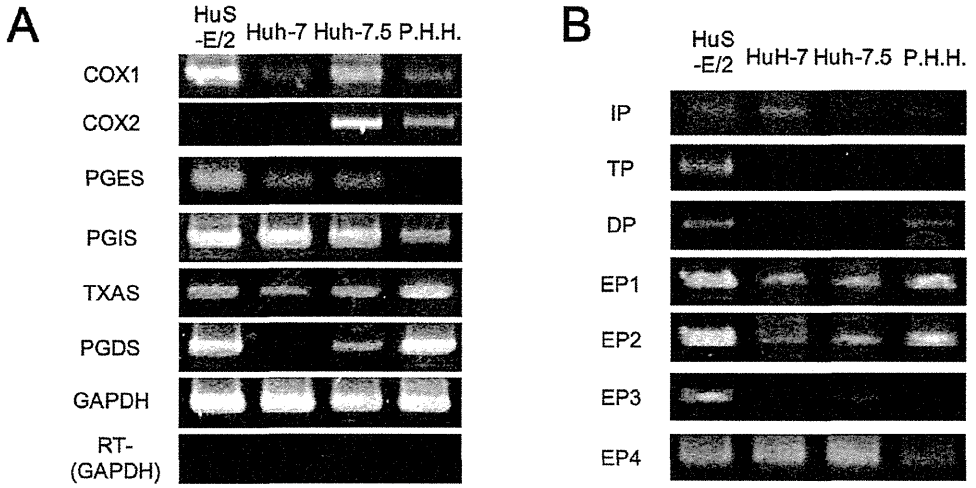

Supplementary Figure 3. Expression of PG synthase and PG-receptor mRNA in immortalized and primary hepatocyte cell lines. (*A* and *B*) mRNA expression levels of various PG synthases and PG receptors in HuS-E/2 cells, Huh-7 cells, Huh-7.5 cells, and primary human hepatocytes were analyzed in RT-PCRs. Representative results from 2 independent experiments are shown.

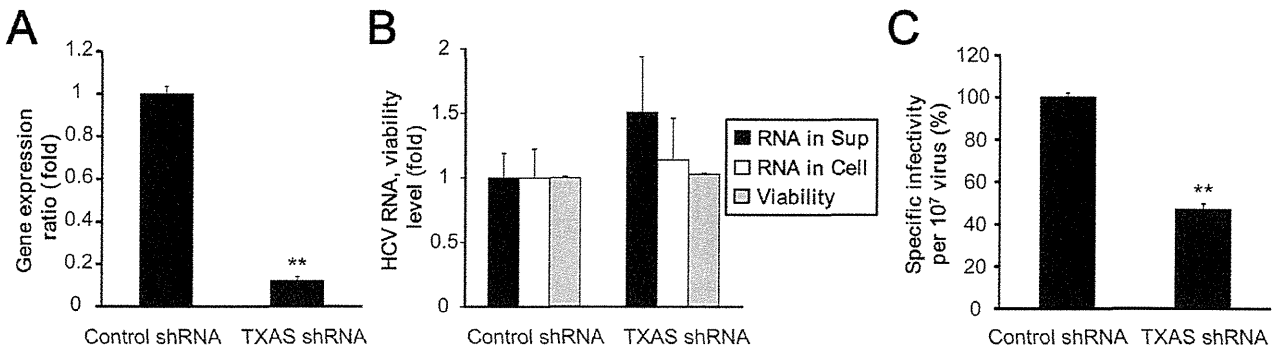

Supplementary Figure 4. Effects of short hairpin RNA (shRNA)-mediated knockdown of TXAS mRNA levels on infectious HCV production. (*A*) Knockdown of TXAS mRNA levels using shRNA. (*B*) Effects of TXAS-specific shRNA on HCV-RNA levels in the HCVcc-producing cell culture system. Levels of HCV RNA in medium (*black bars*) and cells (*white bars*) treated with control or TXAS-specific shRNA were assessed with qRT-PCRs and plotted as amounts relative to results observed with control shRNA–treated cells (control). Mean cell viability ± SD for each sample condition also is plotted (*gray bars*). (*C*) Effects of TXAS-specific shRNA on the infectivity of HCVcc produced using the cell-culture system. **Differs from control, $P < .001$.

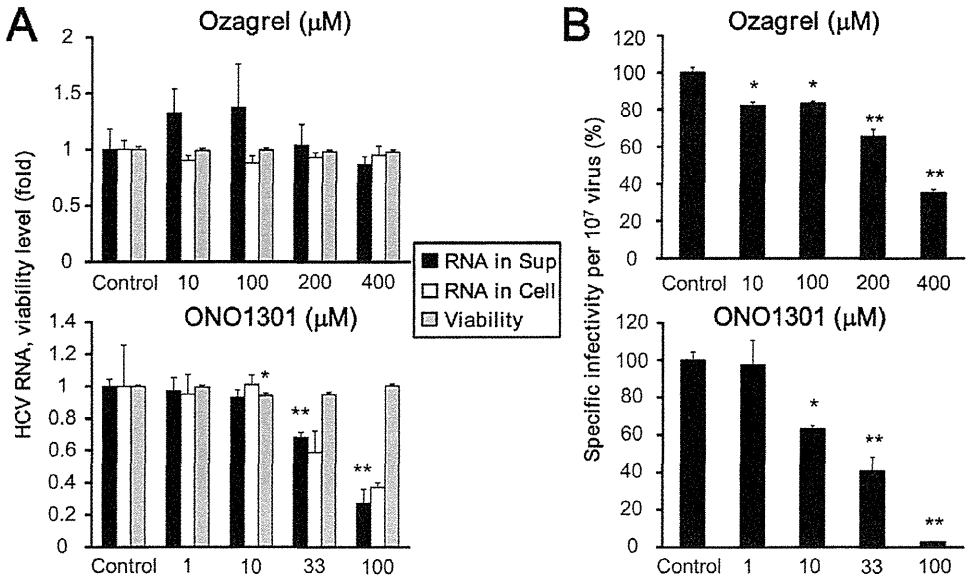

Supplementary Figure 5. Effects of Ozagrel and ONO1301 on the infectivity of HCVcc produced from J6/JFH1-transfected Huh-7.5 cells. (*A*) Effects of Ozagrel (*upper panel*) and ONO1301 (*lower panel*) on HCV-RNA levels in HCVcc-producing cell cultures. Levels of HCV RNA in the medium (*black bars*) and cells (*white bars*) treated with Ozagrel or ONO1301 cells were assessed in qRT-PCRs and plotted as the amount relative to results from untreated cells (control). Mean cell viability ± SD for each sample condition also is plotted (*gray bars*). (*B*) Effects of Ozagrel (*upper panel*) and ONO1301 (*lower panel*) on the infectivity of HCVcc produced in the cell-culture system. *Differs from control, $P < .01$; **differs from control, $P < .001$.

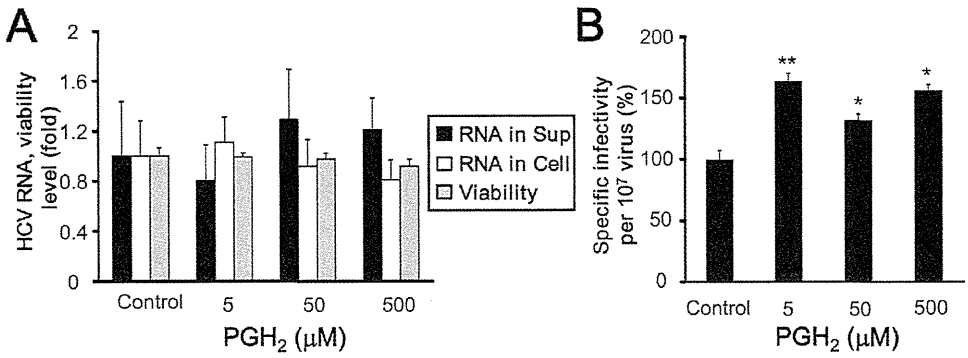

Supplementary Figure 6. Effects of PGH_2 on infectious HCV production. (*A*) Effects of PGH_2 on HCV-RNA levels in the HCVcc-producing cell-culture system. Levels of HCV RNA in medium (*black bars*) and cells (*white bars*) treated with or without PGH_2 were assessed with qRT-PCRs and plotted as amounts relative to results observed with control cells (control). Mean cell viability ± SD for each sample condition also is plotted (*gray bars*). (*B*) Effects of PGH_2 on the infectivity of HCVcc produced using the cell culture system. *Differs from control, $P < .01$; **differs from control, $P < .001$.

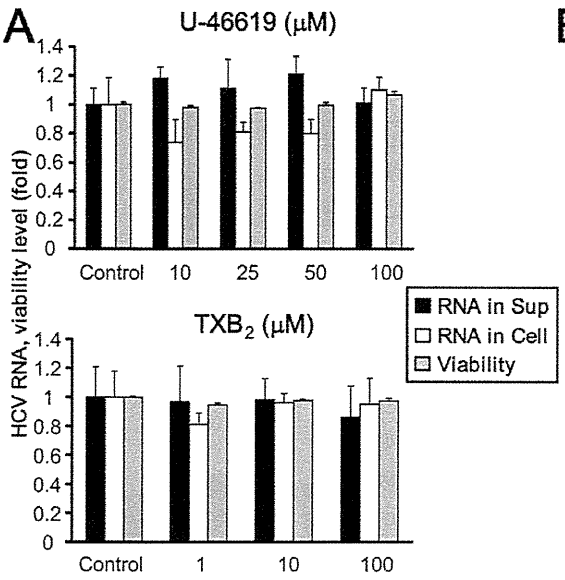

Supplementary Figure 7. Effects of U-46619 and TXB_2 on infectious HCV production. (*A*) Effects of U-46619 (*upper panel*) and TXB_2 (*lower panel*) on HCV-RNA levels in HCVcc-producing cell cultures. Levels of HCV RNA in the medium (*black bars*) and cells (*white bars*) treated with U-46619 or TXB_2 were assessed in qRT-PCRs and plotted as the amount relative to results observed with untreated cells (control). Mean cell viability ± SD for each sample condition also is plotted (*gray bars*). (*B*) Effects of U-46619 (*upper panel*) and TXB_2 (lower panel) on the infectivity of HCVcc produced in the cell-culture system were assessed.

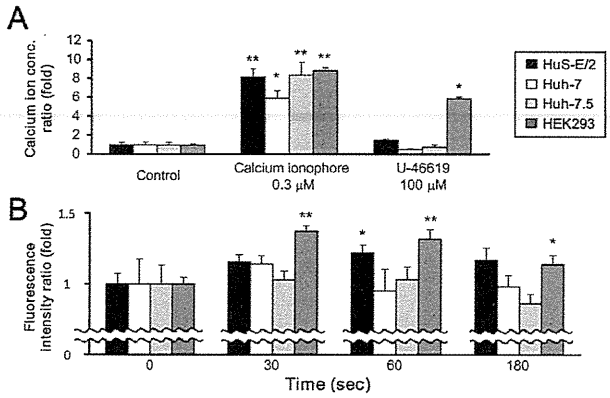

Supplementary Figure 8. Effects of U-46619 on HuS-E/2, Huh-7, Huh-7.5, and HEK293 cell lines via TP. (*A*) Concentrations of intracellular calcium ions were measured in HuS-E/2 (*black bars*), Huh-7 (*white bars*), Huh-7.5 (*gray bars*), and HEK293 (*dark gray bars*) cells treated with or without a calcium ionophore or U-46619. Calcium ion concentrations relative to those in mock-treated cells (control) were determined from triplicate wells in 2 independent experiments and are shown as means ± SD. (*B*) Actin polymerization after U-46619 treatment was measured with fluorescein isothiocyanate (FITC)-labeled phalloidin. *Differs from control, $P < .01$; **differs from control, $P < .001$.

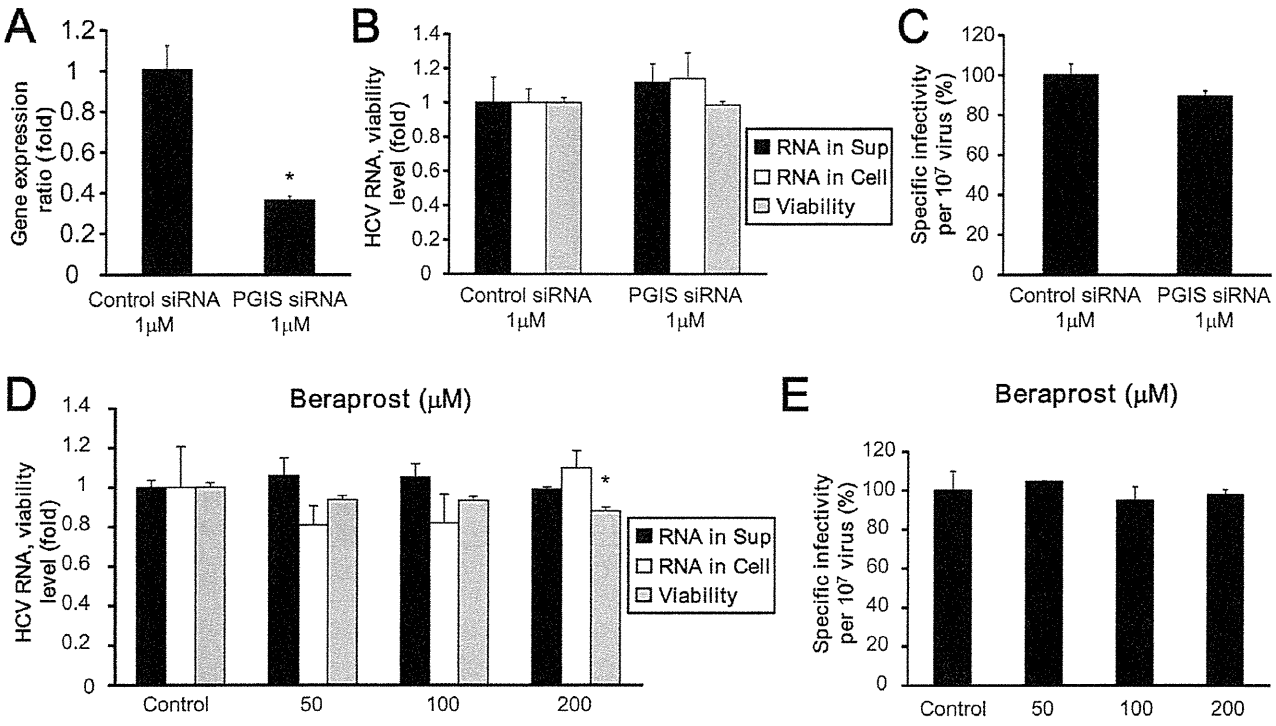

Supplementary Figure 9. Effects of PGI_2 on infectious HCV production. (*A*) siRNA-mediated knockdown of PGIS expression. (*B*) Effects of PGIS-specific siRNA on HCV-RNA levels in HCVcc-producing cell cultures. Levels of HCV RNA in medium (*black bars*) and cells (*white bars*) treated with control or PGIS-specific siRNA were assessed in qRT-PCR and are plotted as amounts relative to results obtained with control siRNA–treated cells (control). Mean cell viability ± SD for each sample condition also is plotted (*gray bars*). (*C*) Effects of PGIS-specific siRNA on the infectivity of HCVcc produced in the cell-culture system. (*D*) Effects of Beraprost on HCV-RNA levels in HCVcc-producing cell cultures. Levels of HCV RNA in medium (*black bars*) and HCVcc-producing Huh-7 cells (*white bars*) treated with Beraprost were assessed in qRT-PCRs and plotted as amounts relative to results obtained with untreated cells (control). Mean cell viability ± SD for each sample condition also is plotted (*gray bars*). (*E*) Effects of Beraprost on the infectivity of HCVcc in culture medium from HCVcc-producing cell cultures were assessed. *Differs from control, $P < .01$.

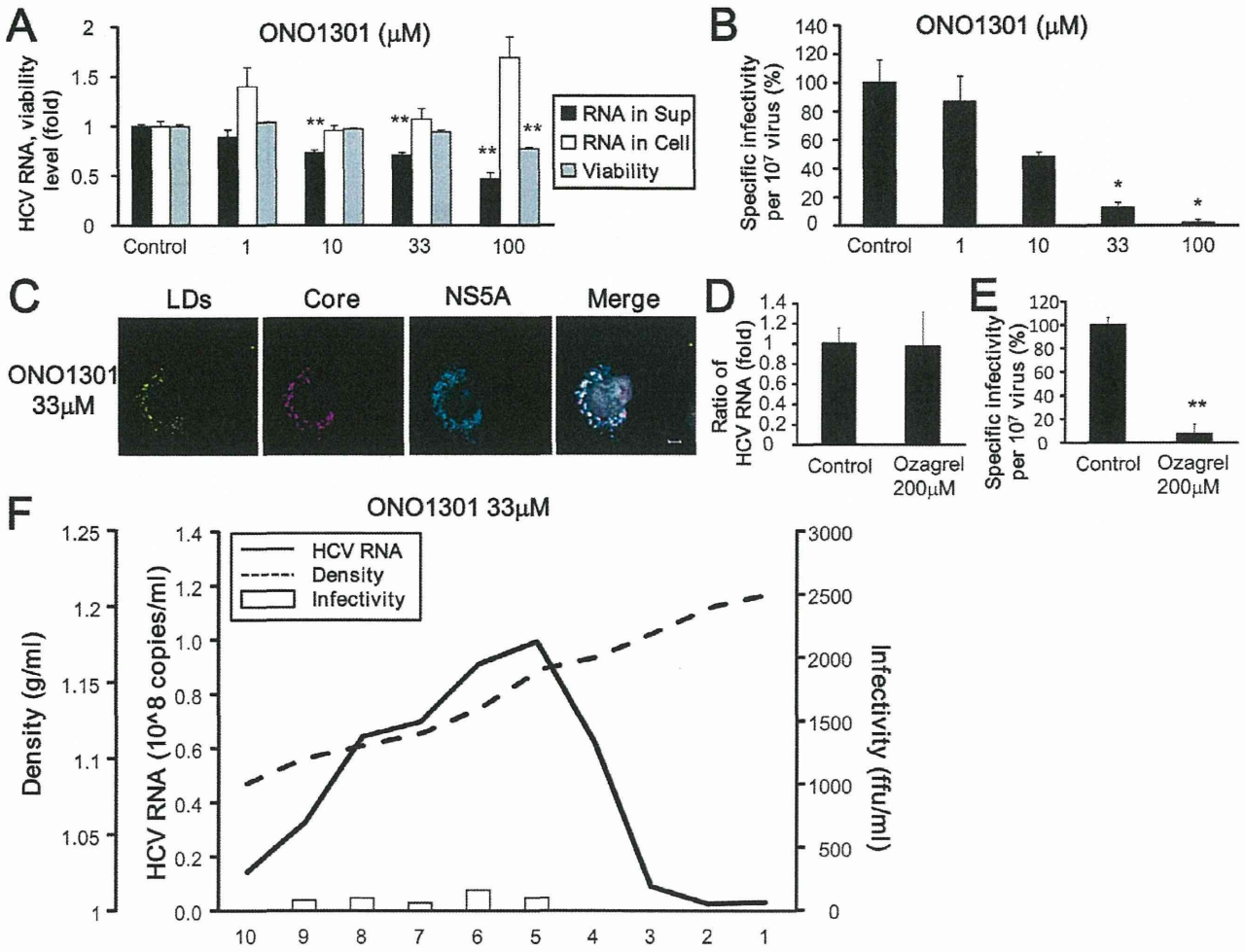

Supplementary Figure 10. Effects of ONO1301 on HCV lifecycle. (*A*) Levels of HCV RNA in medium (*black bars*) and cells (*white bars*) treated with or without ONO1301 were assessed. Mean cell viability ± SD for each sample condition also is plotted (*gray bars*). (*B*) The infectivity of HCVcc in culture medium from HCVcc-producing cell cultures treated with or without ONO1301 was assessed. (*C*) Subcellular locations of HCV core and NS5A proteins around LDs in the presence of ONO1301. Scale bars, 5 μm. (*D* and *E*) Levels and infectivity of intracellular HCV obtained from the cells treated with ONO1301. (*F*) Buoyant density of HCVcc obtained using cells treated with ONO1301. HCV RNA (*solid line*), fraction density (*dotted line*), and HCV infectivity (*white bars*) in each fraction collected by ultracentrifugation. *Differs from control, $P < .01$; **differs from control, $P < .001$.

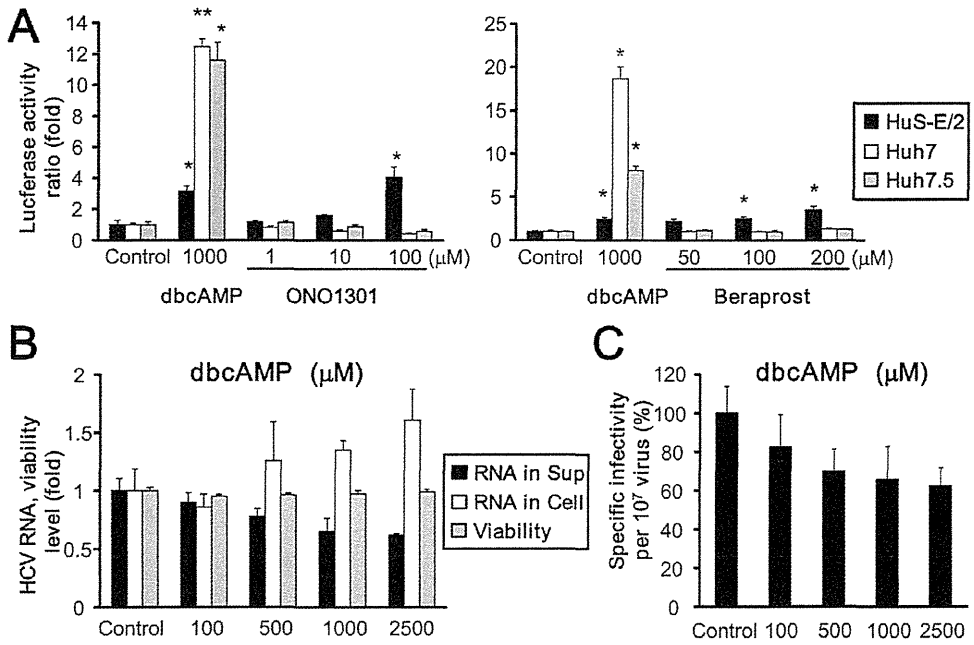

Supplementary Figure 11. Effects of dibutyryl cAMP (dbcAMP) on cell cultures producing JFH1 HCVcc. (*A*) HuS-E/2 (*black bars*), Huh-7 (*white bars*), and Huh-7.5 (*gray bars*) cells were transfected with CRE-Luc plasmid. Then, the luciferase activity in each sample was measured. Values were obtained from quadruplicate wells in 2 independent experiments and are shown as means ± SD. (*B*) Effects of dbcAMP on HCV-RNA levels in HCVcc-producing cell cultures. Levels of HCV RNA in medium (*black bars*) and cells treated with dbcAMP (*white bars*) were assessed in qRT-PCRs and plotted as amounts relative to results obtained with mock-treated cells (control). Mean cell viability ± SD for each sample condition also is plotted (*gray bars*). (*C*) Effects of dbcAMP on the infectivity of HCVcc produced using the cell-culture system. *Differs from control, $P < .01$; **differs from control, $P < .001$.

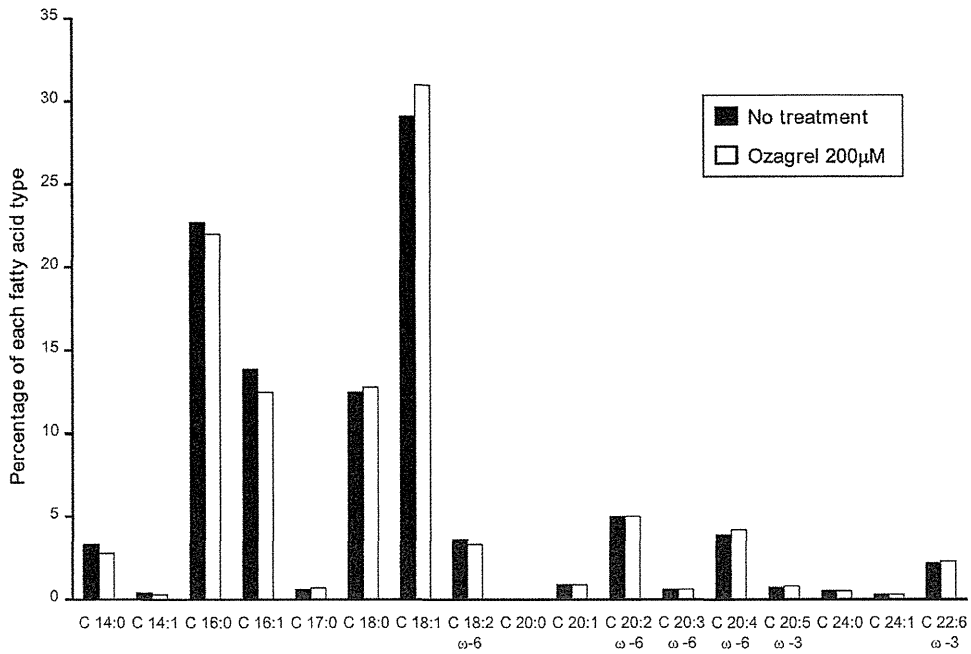

Supplementary Figure 12. Comparison of composition of fatty acids in HCV-infected Huh-7.5 cells with or without Ozagrel treatment.

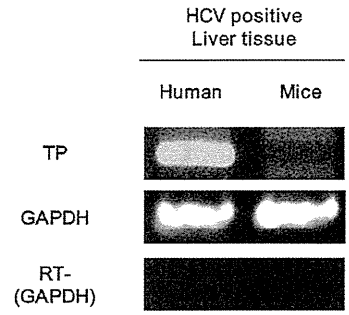

Supplementary Figure 13. Expression of TP mRNA in liver tissues from human patients and chimeric mice infected with HCV.

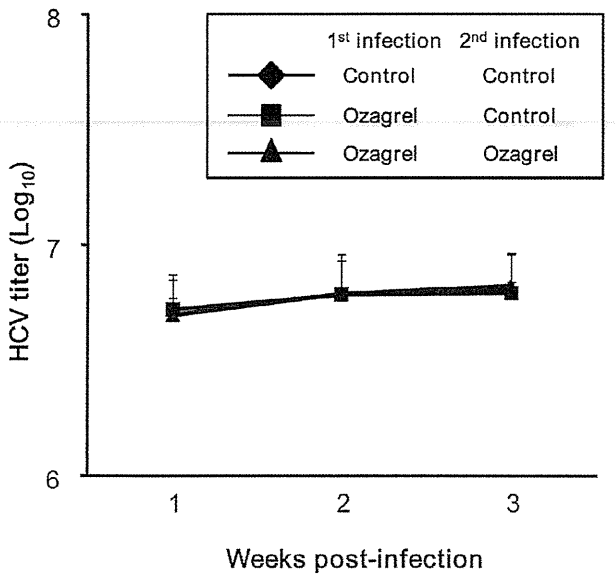

Supplementary Figure 14. Secondary infection of HCV derived from the chimeric mice model. Data are presented as means ± SD for 4 samples.